Helgol Mar Res (2013) 67:83–96
DOI 10.1007/s10152-012-0306-3

ORIGINAL ARTICLE

A functional and morphological approach to evaluate the vertical migration of estuarine intertidal nematodes during a tidal cycle

M. C. Brustolin · M. C. Thomas · P. C. Lana

Received: 22 September 2011 / Revised: 3 April 2012 / Accepted: 12 April 2012 / Published online: 1 May 2012

Abstract We tested herein the hypothesis that exposure time significantly contributes to the vertical distribution profile of nematodes during a tidal cycle as a function of distinct feeding and locomotion behaviors, conditioned by body morphology. We showed that the vertical distribution profile of the slender with filiform tail, numerically dominant *Terschellingia longicaudata* is in fact significantly correlated with sediment changes induced by tidal variation. Conversely, none of the other nematode species showed unequivocal evidence of vertical migration. Horizontal spatial heterogeneity also influenced the vertical distribution of nematode associations, probably as a response to varying temperature and desiccation levels at the sediment surface. The resulting vertical profiles for individual or species groups are a trade-off among locomotory and feeding strategies and concordant morphological adaptations.

Keywords Nematodes · Spatial structure · Locomotion behavior · Feeding strategies · Functional diversity · Tidal flat

Communicated by Heinz-Dieter Franke.

M. C. Brustolin (✉) · P. C. Lana
Centro de Estudos do Mar, Universidade Federal do Paraná, Av. Beira Mar, s/n, Pontal do Paraná 83255-000, Brazil
e-mail: marcobrustolin@gmail.com

M. C. Brustolin · M. C. Thomas
Departamento de Zoologia, Universidade Federal do Paraná, Rua Francisco H. dos Santos s/n, Jardim das Américas, Curitiba, Paraná 81531-980, Brazil

Introduction

Regardless of their predominantly benthic life, meiofaunal animals can be moved or resuspended by water currents due to their small size and preference for the surface sediment layers (Boeckner et al. 2009). However, free-living nematode species can present variable vertical distribution patterns (Maria et al. 2012). The vertical distribution of species belonging to the genus *Sabatieria*, for example, might be more related to the availability of preferred food than with the environmental variations arising from the redox discontinuity layer (Steyaert et al. 2001, 2003). Differing vertical distribution patterns suggest that functional groups or individual nematode species can display distinct migration behaviors as an adaptive strategy to the environmental dynamism, especially in intertidal areas (Steyaert et al. 2001). In particular, variations in the water content are known to affect the locomotion behavior of more "active" nematodes, such as *Enoploides longispiculosus,* which actively captures its food (Steyaert et al. 2001; Gallucci et al. 2005). Thus, biological interactions may play an important role in the vertical spatial segregation of nematode associations. Nematode prey can change their vertical distribution or migrate as a response to predation pressure by top-down control of predaceous nematodes (Maria et al. 2012). In addition, engineering processes caused by other benthic organisms can influence nematode vertical distribution patterns. Bioturbation, bioirrigation, and predation may differently alter vertical distribution of nematode associations (Braeckman et al. 2011a, b).

The ability of nematodes for vertical migration in the sediment depends on their locomotion and feeding strategies. Nematode locomotion behavior is described as undulating, with the length and frequency of body waves

varying as a function of viscosity (Gray and Lissmann 1964; Wallace 1968). Tail shape (Thistle and Sherman 1985; Thistle et al. 1995), size and shape of the body (Soetaert et al. 2002; Vanaverbeke et al. 2004; Schratzberger et al. 2007), and presence of caudal glands (Gingold et al. 2011) may be related to the ability to move and eventually explain differences in distribution patterns. Nematode feeding strategies are also rather variable, and their locomotion behavior may be conditioned by the "mobility" of the food itself, as diatoms and other microorganisms, mainly in the case of nematodes classified as epistrate feeders. Diatoms, *euglenophytes,* and cyanobacteria are able to migrate vertically in the sediment in synchrony with periods of greater or lesser light and tidal exposure (Saburova and Polikarpov 2003; Mitbavkar and Anil 2004). Nematodes are able to follow microphytobenthic migration toward the surface during the low tide (Boaden and Platt 1971).

Although the vertical migration of meiofauna has been widely discussed in the literature (Boaden and Platt 1971; Palmer and Molloy 1986; Fegley 1987), few studies have assessed interspecific differences (Steyaert et al. 2001; Maria et al. 2012) or used statistically significant spatial replication. We describe herein the vertical distribution patterns of nematodes during a tidal cycle in a subtropical intertidal flat. We tested the hypothesis that exposure time during a tidal cycle significantly contributes to the vertical distribution profile of nematodes as a function of distinct feeding and locomotion behaviors, conditioned by body morphology.

Materials and methods

Study area

The experiment was performed in an intertidal flat on Papagaios Island in the euhaline sector of Paranaguá Bay, in southern Brazil (Fig. 1). Local flats are formed by well-sorted fine sand with low organic matter levels (Noernberg et al. 2006) and are often covered with seaweeds such as *Ulva* and *Enteromorpha* (Ulvaceae, Chlorophyta) or diatom biofilms (Lana 2003). Tides are semidiurnal mixed, with a maximum range of around 2 meters. Tidal currents are unidirectional in the rising tides with an average speed of 9 cm s^{-1} (Thomas and Lana 2011). The average salinity is over 30 (Lana et al. 2001). Dynamics of local flats is strongly influenced by the tidal currents, which overcome the effect of the adjacent river flows.

Sampling design

The study was performed during a spring tide, when the tidal flat is exposed nearly twice as long than during the neap tides. Sampling was done every 2 h for 6 h (sampling times T1, T2, T3, and T4), which corresponded to the maximum time of tidal exposure. T1 was performed at the end of the ebb tide, when the tidal flat was still submerged (at 8:30 hours, with 30 cm water cover). The subsequent samplings (T2 and T3) were performed when the flat was fully emerged. T4 was performed during the flood tide, with the flat already submerged (at 14:30 hours, with 50 cm water cover).

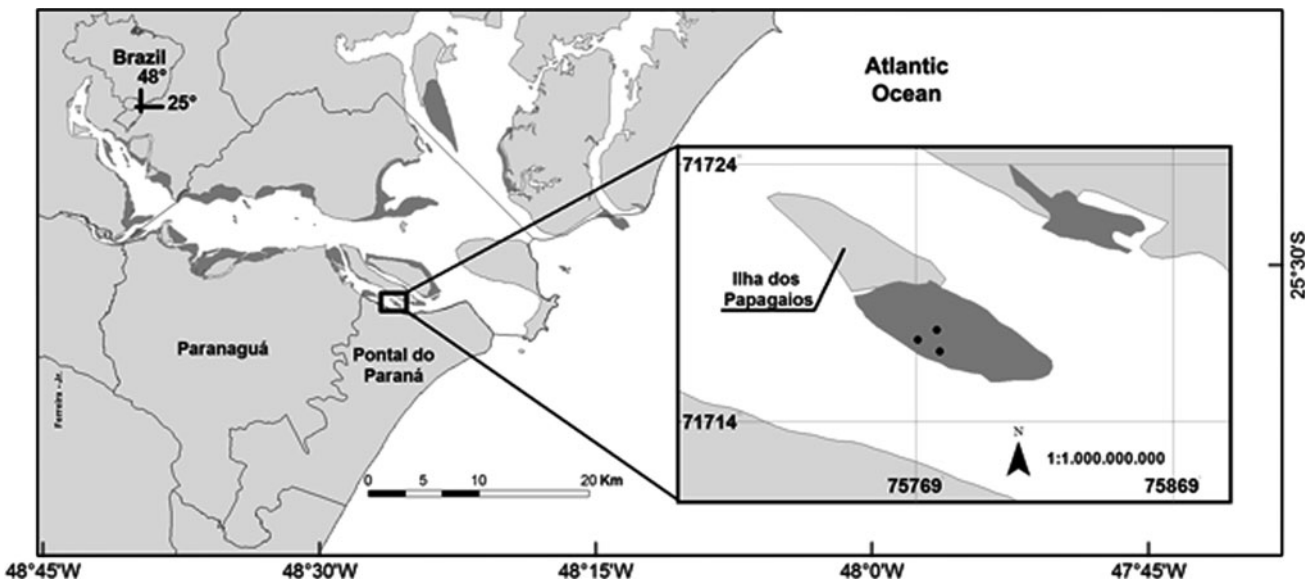

Fig. 1 Map of the estuarine complex of Paranaguá showing the location of the Papagaios tidal flat

Three sites of 1 m^2 were established 50 m apart from each other, in order to ensure proper experimental replication. Each experimental site was subdivided in square areas of 10 cm^2, which were randomly sampled in each sampling time.

Samples were taken with a PVC corer of 2.5 cm in diameter and 5 cm in length, sectioned in ten 0.5 cm strata. In each experimental site and each sampling time, four samples of sediment were taken for meiofaunal analyses (fixed in 4 % formaldehyde), and three for chlorophyll and phaeopigment analyses (stored in a cooler and subsequently frozen at −18 °C). Water content was measured from samples taken at each site. Sediment temperature was measured in situ at each site using a precision digital thermometer with the sensor inserted into each of the strata. Three additional samples, one in each experimental site, were taken for sediment texture analysis.

Sample processing

Biological samples were initially washed through a sieve with a mesh of 63 μm for the removal of formaldehyde. After the washing, the organisms were separated based on their differential densities (Somerfield and Warwick 1996) using a flotation method based on a colloidal silica solution (Ludox TM 50) adjusted to a specific gravity of 1.15 g cm^{-3}.

All nematodes from each stratum were counted under a stereomicroscope. Permanent slides were mounted for 120 organisms. The nematodes were identified using the identification keys from Platt and Warwick (1983, 1988), Warwick et al. (1998) and taxonomic literature.

The pigments were extracted from the sediment samples with 10 ml of 100 % acetone (Strickland and Parsons 1972). The chlorophyll-*a* and phaeopigment concentrations were estimated using the Lorenzen equation (Lorenzen 1967). The water content was obtained by the difference between the wet weight of an aliquot of 3 g of sediment and the dry weight after drying in an oven at 60 °C for 12 h. Total organic matter content (TOM) was determined by oxidation with hydrogen peroxide H_2O_2, and the carbonates were removed by acidification with 0.1 N HCl. Grain-size distribution of the sandy fraction was analyzed using dry sieve technique (% sand = fraction >62 μm) and the fine particle fraction (silt + clay, with particles smaller than 62 μm) followed the pipetting method proposed by Carver (1971). Sediment statistical parameters were calculated using the SysGran software (Camargo 2006). Redox potential discontinuity depth (RPD in cm) was visually estimated as the depth at which sediment color was turned from brown to black.

Data processing

A tri-factorial permutational multivariate analysis of variance PERMANOVA (Anderson 2001, 2005), based on the Euclidean distance matrices, was used for significance testing of the differences between the physicochemical sediment variables over time. Sampling times and strata were treated as fixed factors, the sites as the random factor, and the water content, temperature, and concentrations of chlorophyll-*a* and phaeopigments as the dependent variables. The homogeneity of dispersions was tested with PERMDISP, using distances among centroids calculated both within Sites(Ti) averaged depths and within Ti × St averaged sites groups. Data from the chlorophyll-*a* and phaeopigment concentrations were transformed into log values ($x + 1$) to meet the assumptions of homogeneity of variances.

Nonparametric multivariate methods from the PRIMER v6 software (Clarke and Gorley 2006) were used to correlate species vertical distribution to biological traits presumed to be relevant to locomotion behavior. Times and strata were defined as the fixed factors and the densities of nematodes species as the dependent variables. Bray–Curtis similarity matrices were based on non-transformed abundance and relative frequency data. Nematode species or taxa were classified in 14 categories according to the morphology of the mouth, tail, body shape, body length, and life history strategy (Schratzberger et al. 2007). Buccal morphology was used to recognize the four trophic categories defined by Wieser (1953) as selective deposit feeders (1A), non-selective deposit feeders (1B), epistrate feeders (2A), and omnivorous predators (2B). The morphology of the tail comprises other four categories defined as short/rounded, filiform/elongated, conical, and clavate (Thistle and Sherman 1985; Thistle et al. 1995). Lastly, four categories were recognized based on the body length (<1 mm, 1–2 mm, 2–4 mm, and >4 mm) and two categories based on the body shape (stout with the length/width ratio <18, and slender with the length/width ratio >18) following Soetaert et al. (2002) and Schratzberger et al. (2007).

Temporal variations of associations during the study were visualized through non-metric multidimensional scaling (nMDS) plots. A tri-factorial PERMANOVA, based on the non-transformed Bray–Curtis dissimilarity matrices, was used to significance testing of the differences between the groups, and homogeneity of dispersions was tested with PERMDISP.

The species choice for univariate analysis followed two criteria: (a) the four numerically dominants in the four trophic groups, namely *T. longicaudata*, *S. parasitifera*, *S. pulchra,* and *Viscosia glabra* and (b) one species with a different vertical distribution profile in each trophic group, namely *Daptonema setosum*, *M. chandlleri*, *Gomphionema* sp., and *Euristomina* sp. No selective deposit feeders other than *T. longicaudata* were included on account of their low numbers.

Once the species that contributed the most to the observed differences were identified, a tri-factorial PERMANOVAs was conducted, the sampling times and the strata were used as the fixed factors, the sites as the random factor, and the densities of nematode species as the dependent variable. The homogeneity of variances was examined by PERMDISP. All fauna data were transformed to the fourth root to meet the assumptions.

The PERMANOVAs were based on the mixed linear model below:

$$X_{ijkl} = \mu + Ti_i + St_j + Si(Ti)_{k(j)} + Ti \times St_{ij} + St \times Si(Ti)_{jk(i)} + e_{ijkl} \quad (1)$$

where μ = global average; Ti_i = time factor, fixed with 4 levels; St_j = stratum factor, fixed with 10 levels; $Si(Ti)_{k(i)}$ = site factor, random with 3 levels, nested in time; $Ti \times St_{ij}$ = interaction of the factors time and stratum; $St \times Si(Ti)_{jk(i)}$ = interaction of stratum and site nested in time; e_{ijkl} = error or residue. In case of significant Ti × St interactions, pairwise tests of Ti within Ti × St were performed to investigate which strata differed in time.

Lastly, a canonical correspondence analysis (CCA) was conducted to correlate the variation patterns of the more representative species with the physicochemical variables. The environmental variables were standardized, and the fauna data were log-transformed. The Monte Carlo permutation test was performed to select the environmental variables that significantly explain the variability in the abundance of nematode species ($\infty = 0.05$). A second Monte Carlo permutation test was performed to evaluate the significance of the canonical axes. The CCA and the Monte Carlo permutation tests were carried out in the CANOCO software for Windows (Ter Braak and Smilauer 1998).

Results

Environmental characteristics of the intertidal flat

The Papagaios tidal flat is composed primarily of poorly sorted, very fine to fine sand (Table 1). During the sampling period, the intertidal flat was covered with the green alga *Ulva flexuosa* and presented high densities of the bivalve *Anomalocardia brasiliana*. Redox potential discontinuity depth, varying between 1 and 1.5 cm of depth, was considered as the limit of the sediment surficial layer.

Temperature differed significantly among strata over sites nested in sampling times (St × Si(Ti), pseudo-$F = 7.487$, $P(\text{perm}) = 0.001$) (Table 2).

The temperature profile increased in all analyzed strata over the tidal exposure time. On T1 and T2, highest temperatures were observed in the deeper sediment layers (between 4.0 and 5.0 cm depth). An inverse trend was observed on T3, when the highest recorded temperatures occurred in the surface layers (between 0 and 1.0 cm depth). On T4, the temperature profile of the submerged flat was again similar to T1 and T2 (Fig. 2). The water content differed significantly among strata (pseudo-$F = 7.470$, $P(\text{perm}) = 0.001$) and among sites nested in sampling times (pseudo-$F = 2.437$, $P(\text{perm}) = 0.012$), but not in the tested interaction terms (Table 2). The water content was always higher in superficial sediment layer throughout the experiment (0–0.5 cm depth) although there was a relative increase in the deeper layers (between 2.5 and 3.5 cm depth) on T2. The water content profile on T3 resumed to what was observed before (Fig. 2).

Table 1 Granulometric parameters in each site

	Site 1	Site 2	Site 3
Silt and clay (%)	8.64	7.35	7.15
M. O. (%)	2.30	4.92	1.72
$CaCO_3$ (%)	2.96	3.96	3.42
Median grain size (phi)	3.07	3.13	3.08
Sorting coefficient	Poorly sorted	Poorly sorted	Poorly sorted

Chlorophyll-*a* concentration differed significantly among strata over the sampling times (pseudo-$F = 1.626$, $P(\text{perm}) = 0.050$). Pairwise comparisons showed that on T1, when the tidal flat was submersed, chlorophyll-*a* concentration was significantly higher in 0–0.5 and 0.5–1.0 cm depths, compared with subsequent depths, than in other sampling times. On T2, at 1.0–1.5 and 1.5–2.0 cm depths, when the tidal flat was exposed, chlorophyll-*a* concentration was similar to T1 and significantly higher than in T3 and T4 (Fig. 3).

Phaeopigments concentration differed significantly among strata (pseudo-$F = 8.369$, $P(\text{perm}) = 0.001$) and among sites nested in sampling times (pseudo-$F = 2.279$, $P(\text{perm}) = 0.021$), but not in the tested interaction terms (Table 2). During the ebb tide (T1), when tidal flat was still submersed, phaeopigments concentration was lower in 0- to 0.5- and 0.5- to 1.0-cm strata in comparison with the other sampling times, when the highest concentrations were always recorded in the surface sediment layers (Fig. 3).

Variation patterns in the vertical distribution of nematode associations

The average number of nematodes per site with all layers integrated (5 cm depth) was 3229 ± 1256 ind. 10 cm^{-2}. The total number of identified nematode taxa was 54 with

Table 2 PERMANOVAs pseudo-*F* and *P* values calculated using the Euclidean distance for environmental variables and Bray–Curtis dissimilarity matrices for species and biological traits

	Time		Strata		Si(Ti)		Ti × St		St × Si(Ti)	
	F	*P*(perm)	*F*	*P*(perm)	*F*	*P*(perm)	*F*	*P*(perm)	*F*	*P*(perm)
Temperature (°C)	35.887	0.006	3.243	0.004	81.076	0.001	4.594	0.001	7.487	0.001
Water content (%)	1.647	n/s	7.470	0.001	2.437	0.012	1.485	n/s	1.215	n/s
Chlorophyll-*a* (μg g^{-1})	9.345	0.007	10.021	0.001	7.279	0.001	1.626	0.050	0.779	n/s
Phaeopigments (μg g^{-1})	1.373	n/s	8.369	0.001	2.279	0.021	1.240	n/s	0.619	n/s
Nematode community	1.229	n/s	29.565	0.001	3.224	0.001	1.249	0.042	1.187	0.011
Biological traits matrix	1.243	n/s	21.176	0.001	2.439	0.001	1.190	0.046	1.275	0.001
T. longicaudata	1.222	n/s	26.795	0.001	2.191	0.006	1.439	0.026	1.109	n/s
S. parasitifera	1.256	n/s	25.604	0.001	1.717	0.014	1.201	n/s	1.086	n/s
M. chandlleri	1.220	n/s	17.875	0.001	1.716	0.036	1.198	n/s	0.865	n/s
Gomphionema sp.	0.625	n/s	6.960	0.001	2.743	0.001	0.830	n/s	1.068	n/s
V. glabra	0.363	n/s	9.985	0.001	2.615	0.002	1.203	n/s	1.023	n/s
Eurystomina sp.	1.744	n/s	7.650	0.001	0.928	n/s	0.884	n/s	1.082	n/s
D. setosum	1.740	n/s	12.666	0.001	2.023	0.010	0.950	n/s	1.134	n/s
S. pulchra	1.545	n/s	22.345	0.001	3.497	0.001	1.633	0.004	1.202	0.049

Degrees of freedom of environmental variables: 3, 9, 8, 27, 72, 240 referent to the factors time, stratum, Si(Ti), Ti × St, St × Si(Ti), and error, respectively; $n = 3$. Degrees of freedom of species matrix: 3, 9, 8, 27, 72, 360 referent to the factors time, stratum, Si(Ti), Ti × St, St × Si(Ti), and error, respectively; $n = 4$

an average per site of 29 ± 3 ind. 10 cm^{-2}. *Terschellingia longicaudata, Spirinia parasitifera, Sabatieria pulchra, Metachromadora chandlleri, Pseudochromadora incubans,* and *Gomphionema* sp. accounted for 75.1 % at site 1, 77 % at site 2 and 80.4 % at site 3 of the relative abundance of nematode association (Table 3).

The structure of nematode associations and biological traits matrix differed significantly among strata over sites nested in sampling times St × Si(Ti) (pseudo-$F = 1.187$, $P(\text{perm}) = 0.011$ and pseudo-$F = 1.275$, $P(\text{perm}) = 0.001$, respectively). Therefore, separate nMDS was performed to each site (Fig. 4). SIMPER analysis showed that eight species, *T. longicaudata, S. parasitifera, S. pulchra, M. chandlleri, P. incubans, Gomphionema* sp., *Chromadorina germanica,* and *Anoplostoma viviparum*, accounted together for more than 75 % of dissimilarity among the sampling times across all analyzed strata. Biological traits that most contributed to dissimilarities (>75 % of cumulative percentage) among sampling times across all strata were selective deposit (1A) and epistrate (2A) feeding types, filiform and conical tail shapes, intermediate size classes of adult individuals (1–2 mm and 2–4 mm) and slender and stout body shapes.

We can recognize two different vertical distribution profiles. The first distribution profile was shown by the numerically dominant *T. longicaudata* that is a selective deposit feeder (1A) and has filiform tail, slender body, and size varying between 1 and 2 mm. The second profile was displayed mainly by *S.parasitifera, M. chandlleri, P. incubans,* and *Gomphionema* sp that are epistrate feeders (2A), with conical tails, stout, and slender bodies and size varying between 1 and 2 mm and 2–4 mm (Table 3).

Variation patterns in the vertical distribution of individual species

Only the densities of the numerically dominant *Terschellingia longicaudata* differed significantly among strata over the sampling times (pseudo-$F = 1.439$, $P(\text{perm}) = 0.026$). The pairwise test performed on the interaction term of the sampling times and strata (Ti × St) showed that the average densities were significantly higher in 0–0.5 cm depth at T1 than at the other sampling times. At T4, densities were significantly smaller in the depth of 0.5–1.0 cm and significantly higher in 1.5–2.0 cm depth compared to the other sampling times (Fig. 5).

With the exception of *S. pulchra*, the densities of analyzed species differed significantly among strata and among sites nested in sampling times Si(Ti) but not between the interaction term St × Si(Ti). Thus, vertical distribution patterns were consistent and did not vary among sites (Table 2).

Spirinia parasitifera, Metachromadora chandlleri, and *Gomphionema* sp. are epistrate feeders (2A) with conical tail, but differ in body size and body shape. *S. parasitifera* has a longer body size (between 2-4 mm), and *M. chandlleri* has a stouter body shape. In addition, the three species presented distinct vertical distribution patterns. While the

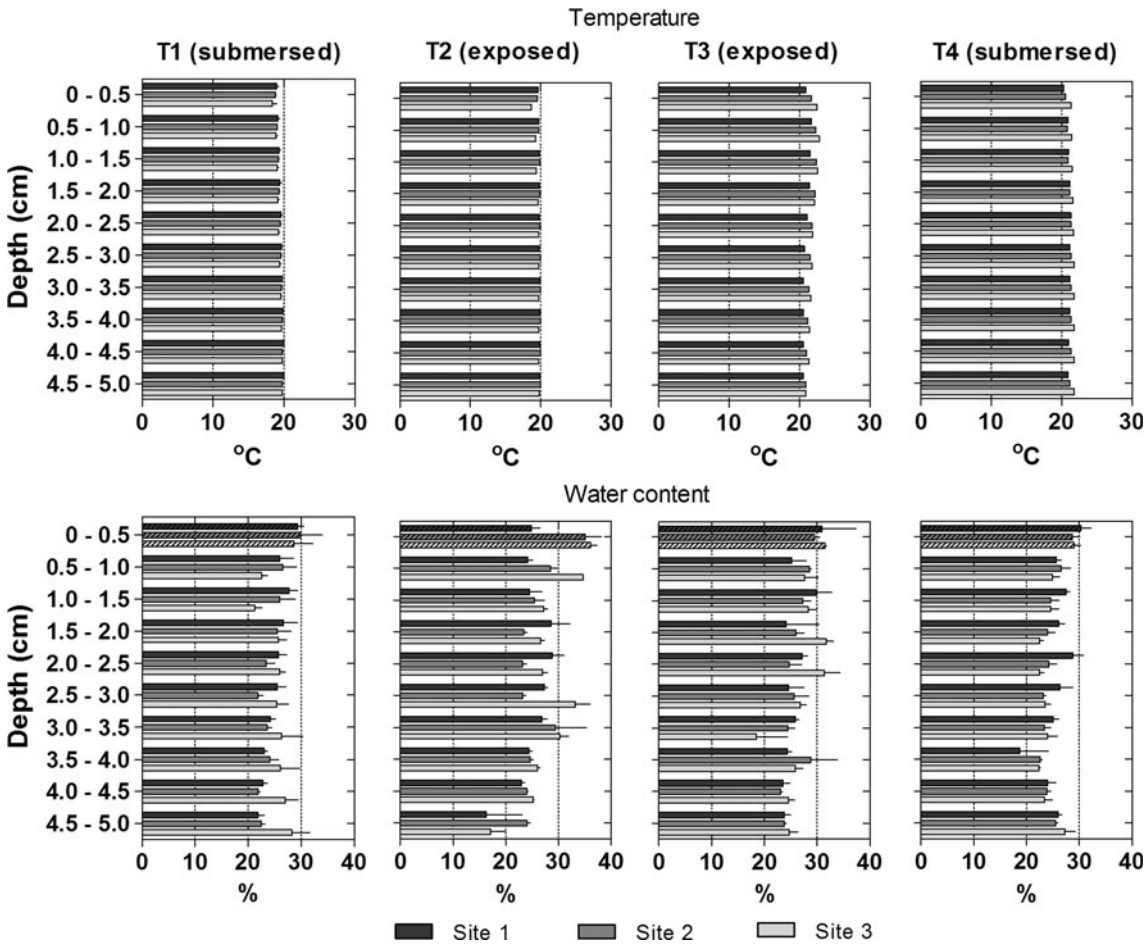

Fig. 2 Vertical profiles of temperature and water content in the three sites over the four sampling times ($n = 3$, average ± SE). *Bars* with *angled dashed lines* were significantly on the pairwise test performed among strata

maximum densities of *S. parasitifera* were recorded in the subsurface layers of the sediment between 0.5 and 1.5 cm (Fig. 5), maximum densities of *M. chandlleri* were recorded in the surface layers, between 0 and 1.0 cm depth. *Gomphionema* sp. occurred preferentially in the deeper layers between 1.5 and 3.5 cm (Fig. 6).

Viscosia glabra and *Eurystomina* sp. are predators (2B) and have slender body shape; however, they differ in characteristics such as the tail shape and body size (filiform and conical, 1–2 and 2–4 mm, respectively). Both species displayed near-surface distributions, although *V. glabra* has a wider vertical distribution profile with maximum densities between 0 and 1.5 cm depth. *Eurystomina* sp. preferentially occurred in the surface layer between 0 and 0.5 cm (Fig. 7).

Sabatieria pulchra and *Daptonema setosum* are non-selective deposit feeders (1B), with a clavate tail, slender body shape, and body size between 1 and 2 mm. The maximum densities of *D. setosum* were recorded in the surface layers of the sediment, between 0 and 1.0 cm. On the other hand, the vertical distribution profile of *S. pulchra* differed significantly among sites nested in sampling times St × Si(Ti) (pseudo-$F = 1.202$, $P(\text{perm}) = 0.049$). Large density variations were recorded among experimental sites (Fig. 8).

Correlation between the species and the environmental variables

The canonical correspondence analysis showed that the species *V. glabra* and *D. setosum,* represented in the positive part of axes 1 and 2, and *M. chandlleri*, represented in the positive part of axis 1 and close to the origin of axis 2, are associated with high concentrations of chlorophyll-*a* and phaeopigments, low levels of sediment water content, and low temperatures. *Eurystomina* sp., represented in the positive part of axis 1 and negative part of axis 2, is associated with high levels of sediment water content and low temperatures. *S. parasitifera* and *S. pulchra,* represented in the negative part of axis 1 and in the positive part of axis 2, are associated with high temperatures, low concentrations of chlorophyll-*a* and phaeopigments, and low levels of

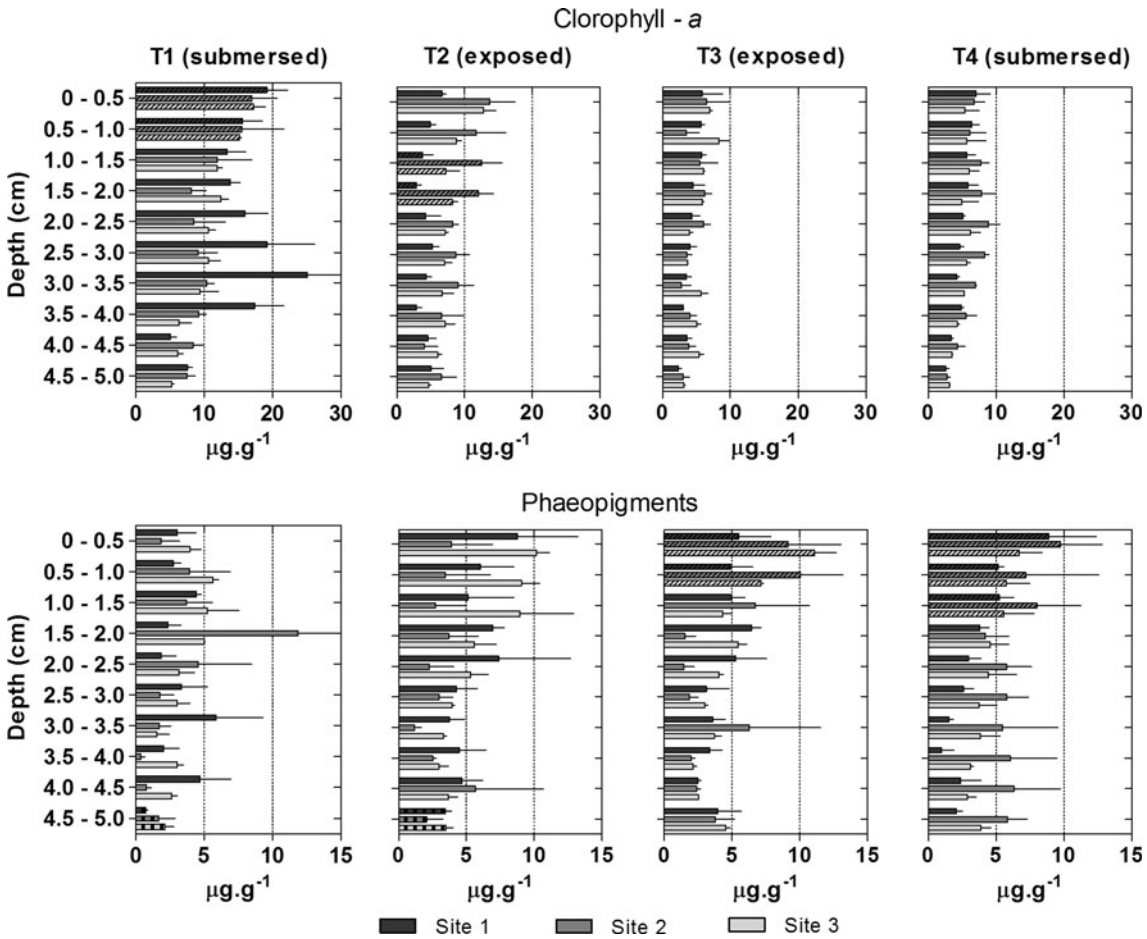

Fig. 3 Vertical distribution of chlorophyll-*a* and phaeopigments concentrations in the three sites during the four sampling times ($n = 3$, average ± SE). *Bars* with *angled dashed lines* were significantly higher on the pairwise test performed among strata over the sampling times (St × Ti) for chlorophyll-*a*. *Bars* with *angled dashed lines* were significantly higher and with *vertical dashed lines* were significantly lower on the pairwise test performed among strata for phaeopigment concentrations

Table 3 Relative abundance (average ± standard error) biological traits of the 15 most abundant nematode species in each of the three experimental sites

	TG	Tail	BL	BS	Site 1	Site 2	Site 3	Total
Terschellingia longicaudata	1A	Fili	1–2	Sl	32.37 ± 42.2	30.65 ± 42.5	34.83 ± 50.5	32.62 ± 2.10
Spirinia parasitifera	2A	Con	2–4	Sl	17.87 ± 23.3	20.26 ± 32.9	20.62 ± 35.0	19.58 ± 1.49
Sabatieria pulchra	1B	Clav	1–2	Sl	9.95 ± 19.1	9.04 ± 11.4	7.61 ± 7.92	8.87 ± 1.18
Metachromadora chandleri	2A	Con	1–2	St	6.56 ± 6.14	8.40 ± 6.71	7.58 ± 6.67	7.51 ± 0.92
Pseudochromadora incubans	2A	Con	>1	Sl	4.45 ± 6.24	5.33 ± 7.22	4.20 ± 5.75	4.66 ± 0.60
Gomphionema sp.	2A	Con	1–2	Sl	3.95 ± 8.59	3.32 ± 3.77	5.57 ± 9.88	4.28 ± 1.16
Chromadorina germânica	2A	Clav	>1	Sl	3.22 ± 7.61	1.17 ± 3.22	1.21 ± 1.68	1.87 ± 1.17
Paradontophora paragranulifera	1B	Fili	1–2	Sl	2.54 ± 3.37	2.76 ± 5.78	1.71 ± 3.12	2.34 ± 0.56
Daptonema setosum	1B	Clav	1–2	Sl	2.47 ± 3.31	3.67 ± 3.75	2.76 ± 4.64	2.97 ± 0.62
Anoplostoma viviparum	1B	Fili	1–2	Sl	2.25 ± 5.23	2.17 ± 5.53	2.06 ± 3.91	2.16 ± 0.10
Viscosia glabra	2B	Fili	1–2	Sl	2.09 ± 3.29	2.28 ± 3.35	2.20 ± 2.79	2.19 ± 0.09
Neochromadora bonita	2A	Con	>1	Sl	1.65 ± 3.83	1.06 ± 1.82	1.04 ± 1.66	1.25 ± 0.35
Paracanthonchus sp1.	2A	Con	1–2	Sl	1.16 ± 2.36	0.76 ± 0.89	0.93 ± 1.58	0.95 ± 0.20
Eurystomina sp.	2B	Con	2–4	Sl	1.13 ± 1.12	1.71 ± 3.56	1.34 ± 2.02	1.39 ± 0.29

TG trophic group, *Tail* tail shape (*Fili* filiform, *Con* conical and *Clav* clavate); *BL* body length in millimeters; *BS* body shape (*St* stout and *Sl* slender)

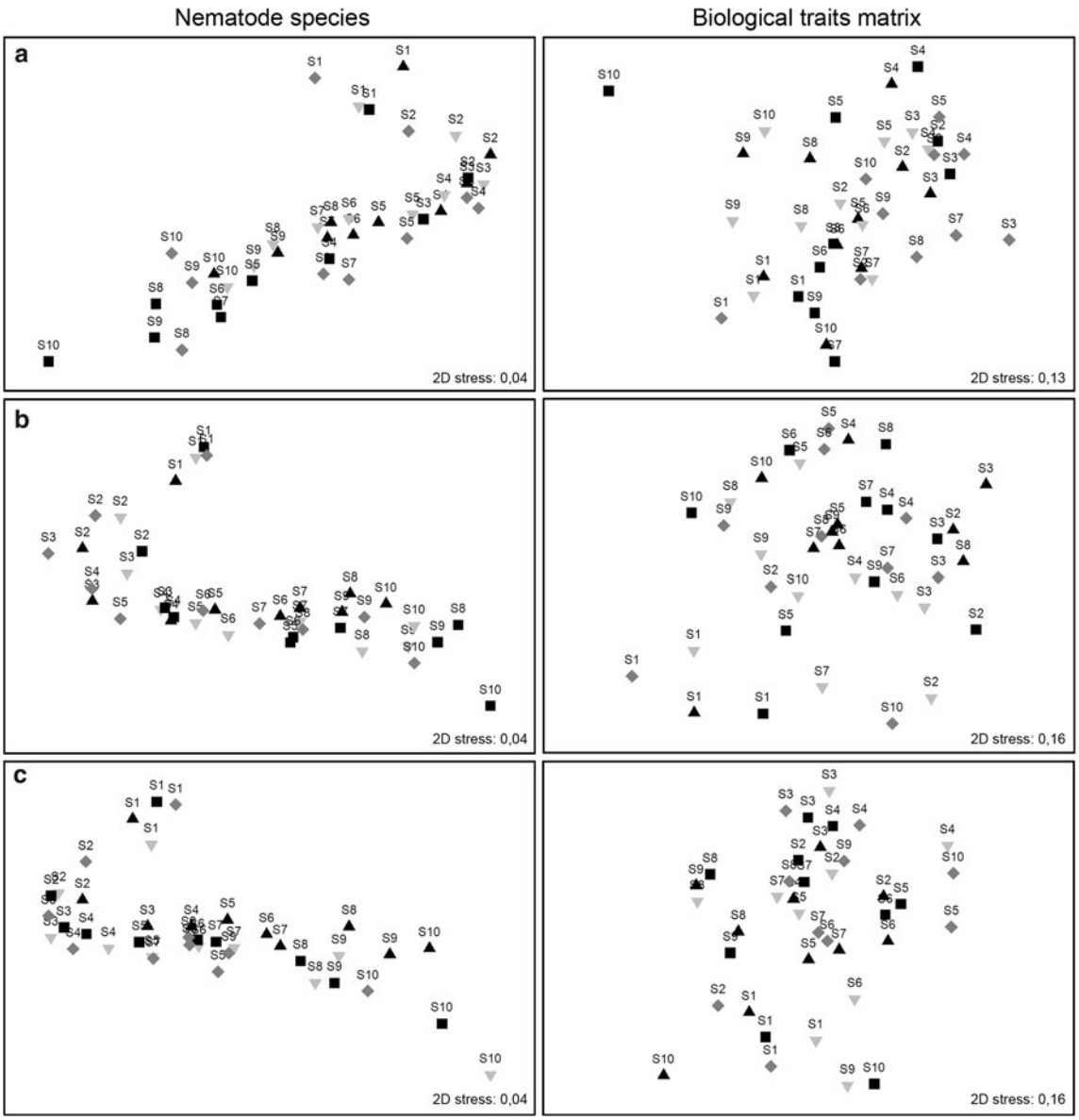

Fig. 4 Non-metric multidimensional scaling (nMDS) based on the Bray–Curtis similarity matrices prepared from the average densities of nematode species and their biological traits in each of the three sites (sites: site 1 = a; site 2 = b; site 3 = c; times: T1 = *black triangles*; T2 = *gray triangles*; T3 = *black squares*; T4 = *dark gray diamonds*; stratum: S1; S2; S3; S4; S5; S6; S7; S8; S9; S10)

sediment water content. *T. longicaudata*, represented in the negative part of axis 1 and close to the origin of axis 2, and *Gomphionema* sp., represented in the negative part of axes 1 and 2, are both associated with low concentrations of chlorophyll-*a* and phaeopigments, low levels of sediment water content, and low temperatures (Fig. 9).

The environmental variables included in the model, with the exception of temperature, explain the significant variability in the densities ($P < 0.05$) of the nematode species (Table 4). The first two axes of the CCA explain 97 % of the relationships between the fauna and the environmental variables. The Monte Carlo permutation test indicated that the explanation of the axes is significant ($P = 0.005$).

Discussion

Our study showed that only the vertical distribution profile of the numerically dominant *T. longicaudata* was unequivocally altered by varying exposure during a tidal cycle. The hypothesis that exposure time during a tidal cycle significantly contributes to the vertical distribution profile of nematodes as a function of distinct feeding and locomotion behaviors, conditioned by body morphology was thus only partially supported.

Two distinct behaviors were displayed by two different species groups. The first pattern was displayed by active species with filiform tail, slender body shape, and body size

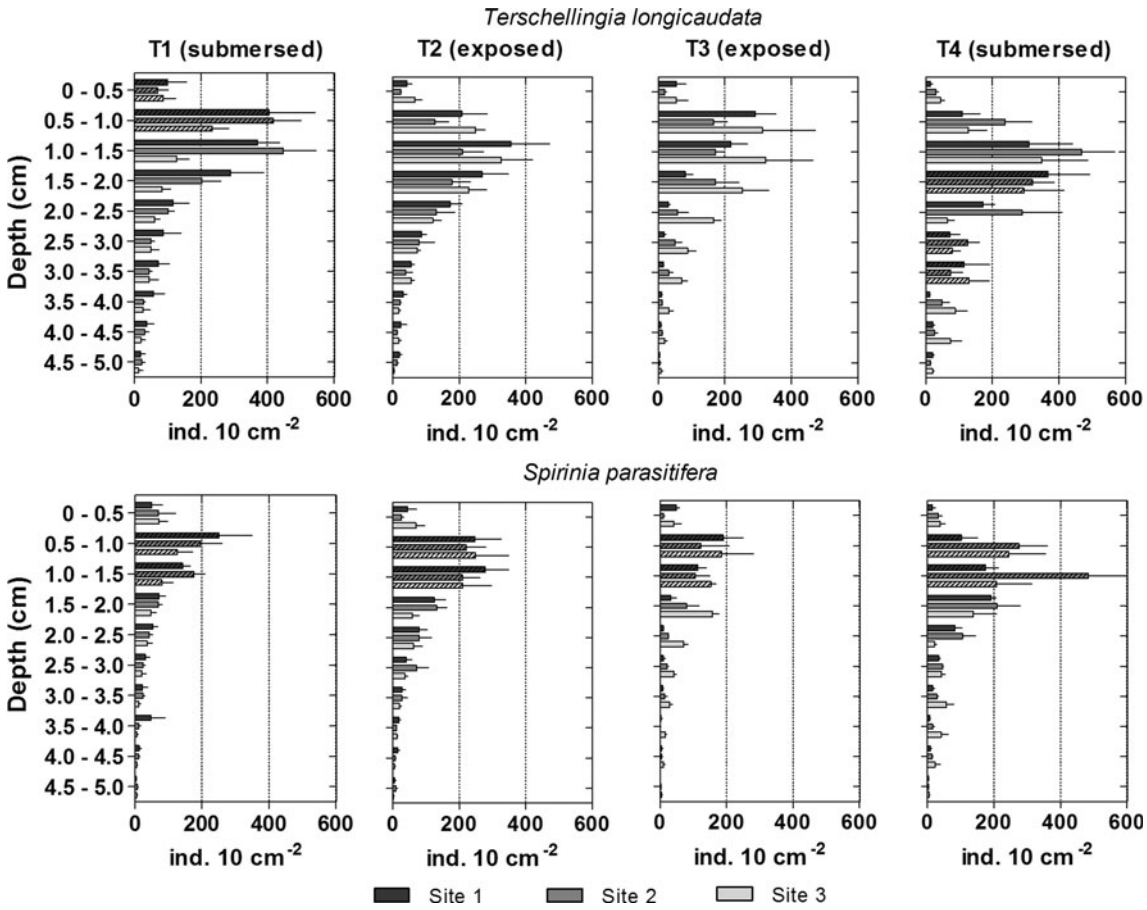

Fig. 5 Vertical distribution of the average densities of nematode species *Terschellingia longicaudata* and *Spirinia parasitifera* in the three sites, during the four sampling times ($n = 4$, average ± SE). *Bars* with *angled dashed lines* were significantly higher on the pairwise test performed among strata over the sampling times (St × Ti) for *T. longicaudata* and among strata for *S. parasitifera*

between 1 and 2 mm, which performed vertical migration. Tail shape, size, and shape of the body are well recognized as relevant to explain the ability of locomotion in nematodes (Thistle and Sherman 1985; Soetaert et al. 2002; Schratzberger et al. 2007). Species belonging to this group also share thin cuticles. Boaden and Platt (1971) suggested that the species with thinner cuticles are less tolerant to episodic desiccation and tend to migrate to deeper sediment layers. Their migration behavior can be affected by changes in the temperature profiles, more variable mainly in the surface sediment layers, between 0 and 1.5 cm. This was mainly due to the direct impact of the solar radiation and the changes in the local albedo as a tidal exposure function.

The second group, dominant between 0 and 0.5 cm depth, was composed by epistrate feeders (2A), with conical tail, slender body shape, and body size between 1 and 2 mm. These species did not display vertical migration though they share some traits with the first group, such as size and body shape, which facilitate locomotion in the interstitial spaces. Their feeding behavior can explain their greater concentration or restriction to the surface strata. Boaden and Platt (1971) and Steyaert et al. (2001) suggested that the vertical distribution of epistrate-feeder nematodes could be related to the movement of the *microphytobenthos,* which is able to migrate vertically into the sediment in synchrony with periods of greater or lesser tidal and light exposure. However, the epistrate-feeder species did not show any clear trends of vertical migration during the tidal cycle, despite their locomotory abilities. This pattern is in accordance with the behavior of microphytobenthic preys, which remained in the surface layers. Rather than to vertical migration, the differences in concentrations of cloroplastic pigments among sampling times were due to high small-scale variability possibly caused by feeding and bioturbation by the bivalve *Anomalocardia brasiliana.* Despite significant variations in pigments content in experiments with the bivalve *Alba alba,* bioturbation activity is probably limited to feeding and sediment reworking and does not consist of deep organic matter burial (Braeckman et al. 2011a, b).

The numerically dominant species, *T. longicaudata,* migrated to deeper layers of the sediment during emersion

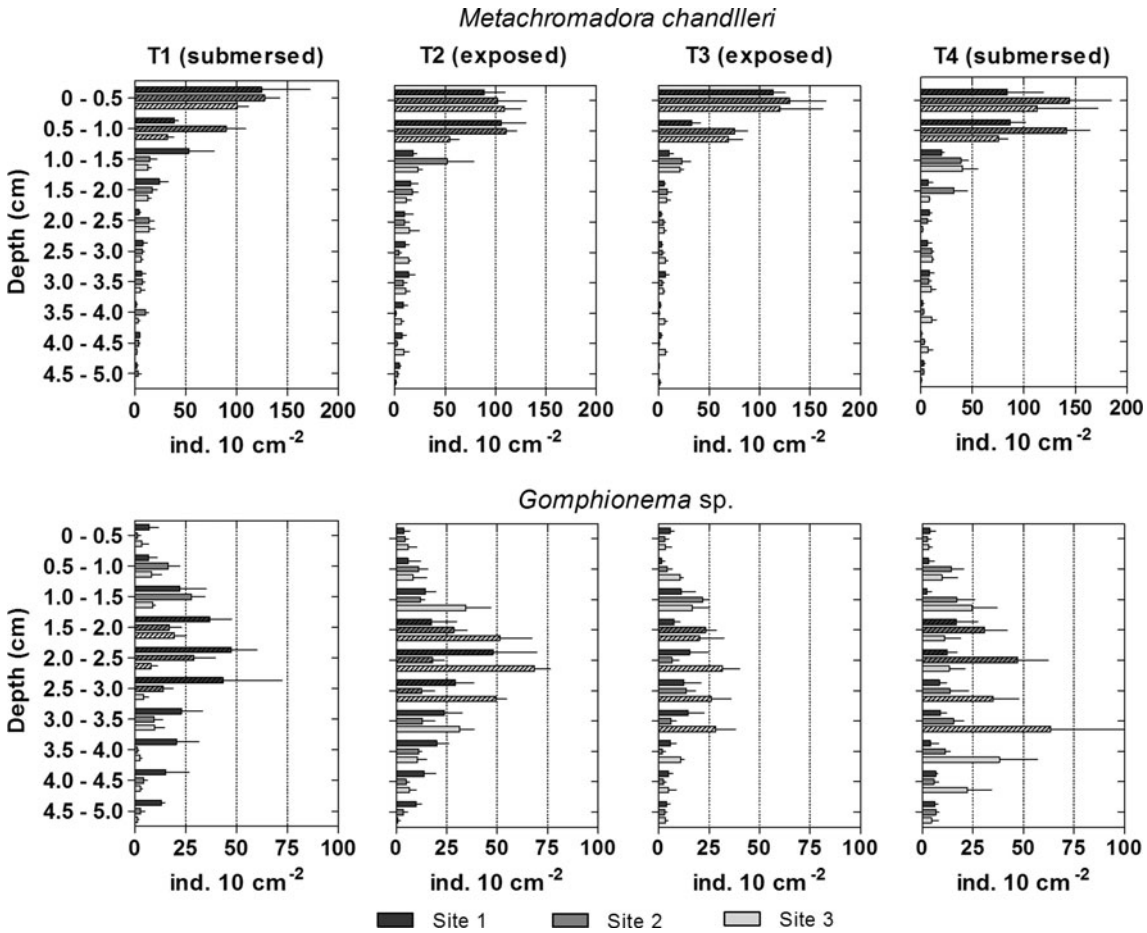

Fig. 6 Vertical distribution of the average densities of nematode species *Metachromadora chandlleri* and *Gomphionema* sp., in the three sites, during the four sampling times ($n = 4$, average ± SE). *Bars* with *angled dashed lines* were significantly higher on the pairwise test performed among strata

periods. The intensification of this migration behavior at T4, just after the flood tide, stresses the importance of the tidal currents and their erosive potential on changing nematode vertical distribution patterns, as suggested by Boaden and Platt (1971), Fegley (1987), Steyaert et al. (2001), Gallucci and Netto (2004). This species displays the feeding strategies and body characteristics that favor an active migrating behavior. Soetaert et al. (2002) correlated smaller body size and filiform shape with greater mobility described. Vertical segregation of nematode predators and preys may also be a function of predation pressure and top-down control on nematode associations (Maria et al. 2012). The search for different food items can be an additional motivation for migration. Moens et al. (1999) reported that selective deposit feeder nematodes are extreme specialists and respond differently to the quality and quantity of food.

Spirinia parasitifera and Metachromadora chandlleri did not display vertical movements, but showed a zonation pattern, concentrating in more surficial layers, probably due to their reduced locomotion abilities because of their body length (in the case of *S. parasitifera*) or body shape (in the case of *M. chandleri*). These conditions were seen as adaptations against predation (Soetaert et al. 2002). In addition, their tolerance to temperature variations and their food preferences may be related to this behavior. On the other hand, *Gomphionema* sp concentrated in the deeper layers of the sediment probably due to a lesser tolerance to sediment variations and a better locomotion capacity.

Viscosia glabra and *Eurystomina* sp. are omnivores/predators (2B) and share a slender body shape, although they differ in the size and shape of the tail (1–2 and 2–4 mm, conical and filiform, respectively). No evidence of vertical movement behavior was observed for these two species, but *V. glabra* displayed a wider vertical distribution profile. *V. glabra* is more able to move through more compacted sediments because it is smaller than *Eurystomina* sp., besides possessing a filiform tail and slender body. Spending less energy in foraging during the emersion periods and preying upon smaller preys can be advantageous. *Eurystomina* sp. are larger animals, and their

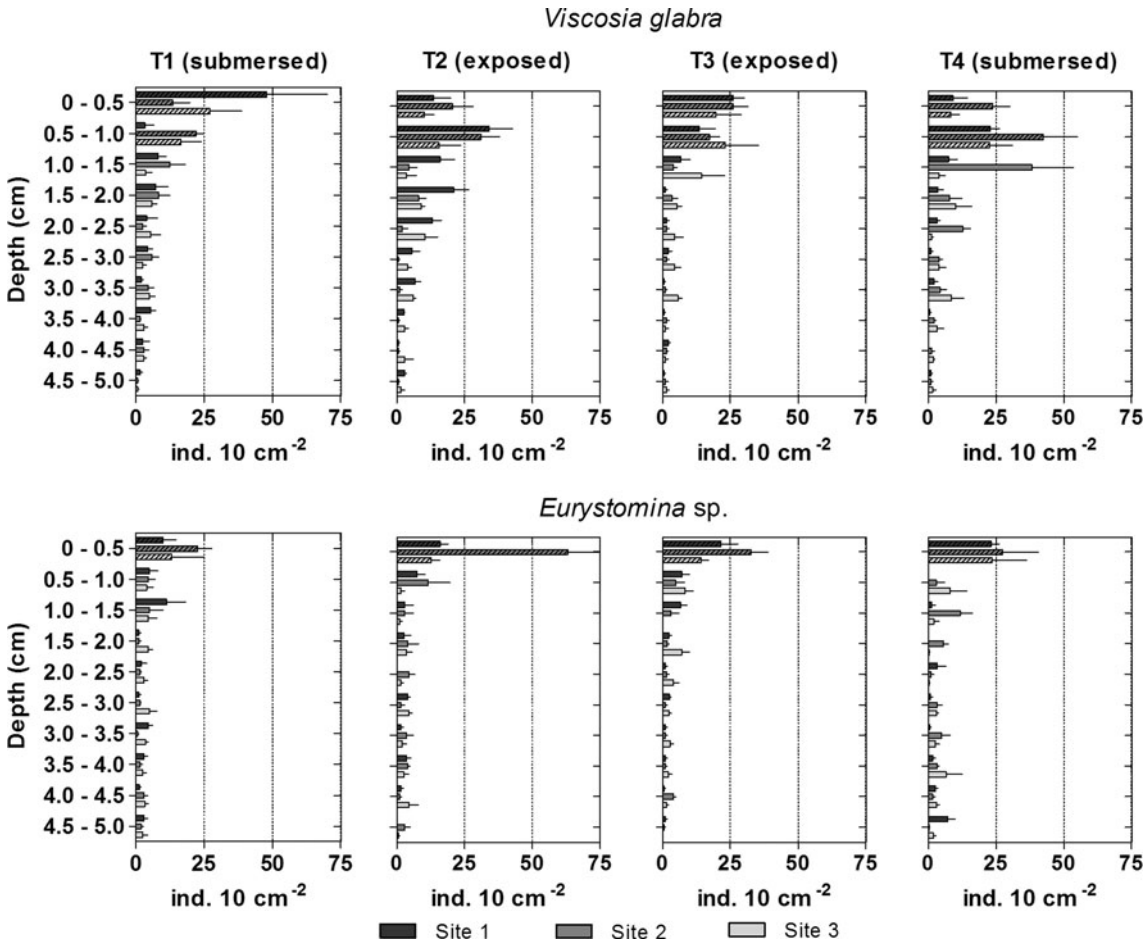

Fig. 7 Vertical distribution of the average densities of nematode species *Viscosia glabra* and *Eurystomina* sp., in the three sites, during the four sampling times ($n = 4$, average ± SE). *Bars* with *angled dashed lines* were significantly higher on the pairwise test performed among strata

motility is facilitated by higher water content in the surface layer. Prey capturing rates have been shown to be positively correlated with the sediment water content (Gallucci et al. 2005). Water content was more stable in the surface layers, probably because of the low permeability of fine sediments and the roughness of the sediment surface, which led to the formation of puddles over the entire tidal flat area.

Although *S. pulchra* presented a wider vertical distribution than *D. setosum,* both are non-selective deposit feeders (1B) and share clavate tail shape, body size between 1 and 2 mm, and slender body shape. The wider range of vertical distribution can be competitive advantageous for *S. pulchra* that is well-known resistant to anoxic and sulphydric conditions and is able to exploit the available food resources at deeper sediment layers (Steyaert et al. 2003, 2005). On the other hand, the vertical distribution of *D. setosum* did not vary significantly among sites. The species always remained in the surface layers of the sediment. This behavior may be related to a feeding preference for diatoms (Steyaert et al. 2001; Moens et al. 2005), an increased tolerance to changes in sediment characteristics, resulting from a well-developed cuticle (Boaden and Platt 1971), and the adaptive response to the action of currents in events of submersion. This species possesses caudal glands that help in both the movement and adhesion to the substrate.

Although the spatial variability of the meiofauna is relatively well documented on small scales (Pinckney and Sandulli 1990; Azovsky et al. 2004; Somerfield et al. 2007), studies on the vertical migration of marine nematodes with a statistically relevant spatial replication have not been previously performed. By incorporating meiofaunal spatial variability in our model for testing a working hypothesis, it was possible to recognize whether the processes of nematode migration occurred recurrently in the tidal flat as a whole or whether these processes were punctual or random. A clear trend of migration to deeper sediment layers during emersion periods was displayed only by the numerically dominant *T. longicaudata*. The vertical distribution profiles of the nematode association as a whole were not homogeneous among the sampling sites

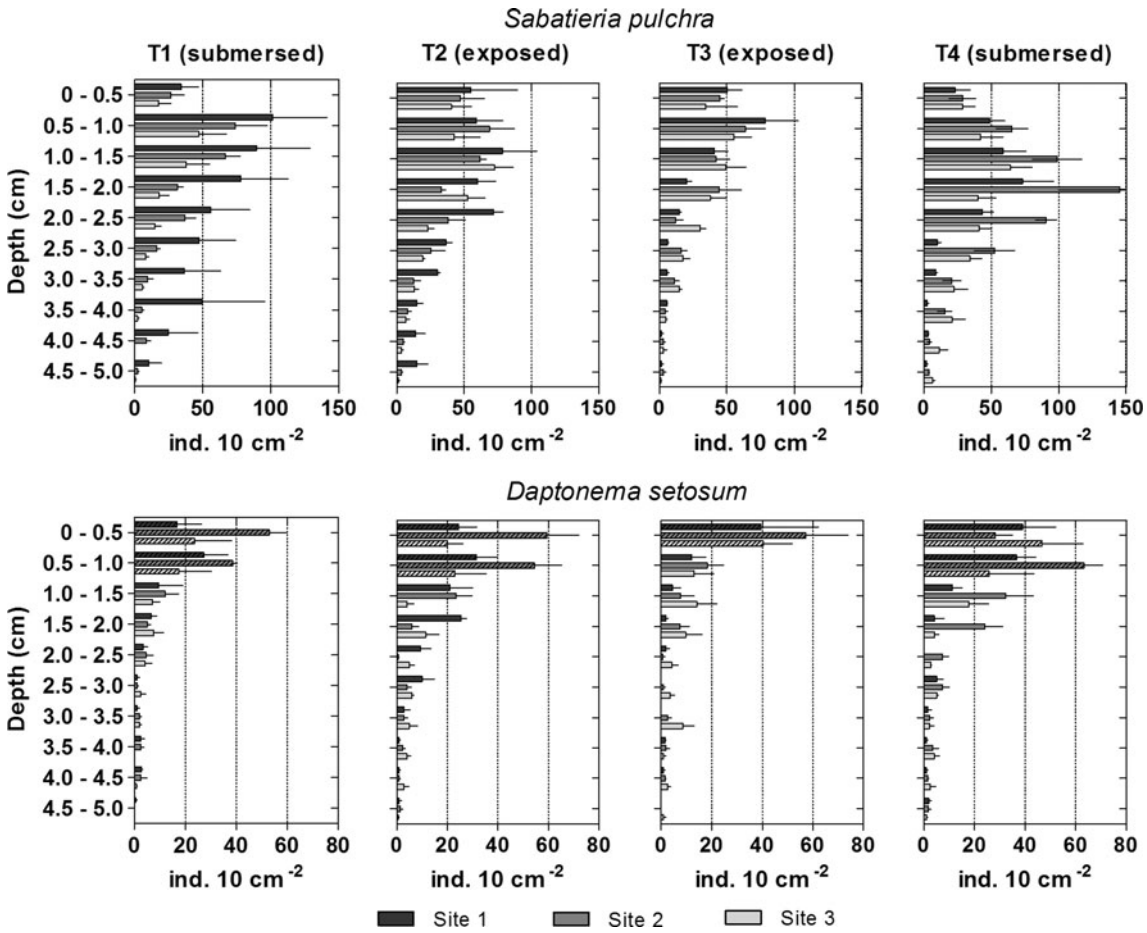

Fig. 8 Vertical distribution of the average densities of nematode species *Sabatieria pulchra* and *Daptonema setosum*, in the three sites, during the four sampling times ($n = 4$, average ± SE). *Bars* with *angled dashed lines* were significantly higher on the pairwise test performed among strata

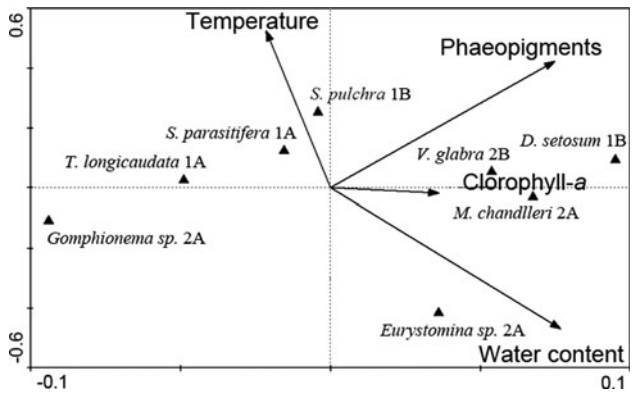

Fig. 9 Graphical representation of the canonical correspondence analysis (CCA), showing the distribution of the mean densities of nematode species (represented by *triangles*) in relation to the environmental variables (represented by *arrows*); $n = 3$

due to spatial variations in population densities. These short-scale variations in horizontal distribution may reflect distinct aggregation and dispersal patterns among the species (Somerfield et al. 2007). Distribution patterns can be modified by the erosive potential of the waves and tide currents (Gallucci and Netto 2004), chemical changes caused by the death and decomposition of organisms (Ólafsson 1992), bioturbation and bioirrigation engineering (Pinto et al. 2006; Braeckman et al. 2011a, b), competition with the macrofauna for food (Ólafsson 2005), preferential selection of food (Gallucci et al. 2005; dos Santos et al. 2008; Franco et al. 2008), and the differing locomotion ability of the species (Gingold et al. 2011).

Table 4 Statistical significance of the environmental variables included in the canonical correspondence analysis (Monte Carlo permutation test, number of permutations = 999)

	F	*P* value
Temperature	1.24	n/s
Water content	12.32	0.001
Phaeopigments	6.64	0.001
Chlorophyll-*a*	3.29	0.014

Despite its potential ecological relevance, the analysis of vertical migration of marine nematodes at the functional groups level can mask the variation patterns of individual species. Our results showed that the vertical distribution profile of a slender with filiform tail, numerically dominant free-living nematode is in fact significantly correlated with sediment changes induced by tidal variation. Conversely, body morphology and feeding strategies may restrict the locomotion of most of the other associated nematode species. We provide strong evidence for morphological and functional differentiation in free-living nematode species across a vertical sediment profile in a subtropical tidal flat subject to significant variation in sediment parameters during a tidal cycle. The resulting vertical profiles for individual or species groups are a trade-off among locomotory and feeding strategies and concordant morphological adaptations.

Acknowledgments We thank three anonymous reviewers for their helpful comments and suggestions. Our thanks also to Nice Shindo for the English translation and helpful comments, to our colleagues and friends Sergio Antonio Netto (Laboratório de Ciências Marinhas, Universidade do Sul de Santa Catarina), Mauricio Garcia de Camargo, Leonardo Sandrini-Neto, Maikon Di Domenico and Verônica Maria de Oliveira (Centro de Estudos do Mar, Universidade Federal do Paraná) for their generous help and advice. Ana Carolina dos Passos, Augusto Luiz Ferreira-Jr., Renato Luiz Bot Neto, Barbara Maichak de Carvalho, Raissa Nogueira, and Diógenes Magno Laube were most helpful during field sampling and sample processing. This study was supported by the Brazilian National Council for Technological and Scientific Development (CNPq), which provided fellowships and grants for the authors.

References

Anderson MJ (2001) A new method for non-parametric multivariate analysis of variance. Austral Ecol 26:32–46

Anderson MJ (2005) PERMANOVA: a FORTRAN computer program for permutational multivariate analysis of variance. Department of Statistics, University of Auckland

Azovsky AI, Chertoprood ES, Saburova MA, Polikarpov IG (2004) Spatio-temporal variability of micro- and meiobenthic communities in a White Sea intertidal sandflat. Estuar Coast Shelf Sci 60:663–671

Boaden PJS, Platt HM (1971) Daily migration patterns in an intertidal meiobenthic community. Thalassia Jugos 7:1–12

Boeckner MJ, Sharma J, Proctor HC (2009) Revisiting the meiofauna paradox: dispersal and colonization of nematodes and other meiofaunal organisms in low- and high-energy environments. Hydrobiologia 624:91–106

Braeckman U, Van Colen C, Soetaert K, Vincx M, Vanaverbeke J (2011a) Contrasting macrobenthic activities differentially affect nematode density and diversity in a shallow subtidal marine sediment. Mar Ecol Prog Ser 422:179–191

Braeckman U, Provoost P, Moens T, Soetaert K, Middelburg JJ, Vincx M, Vanaverbeke J (2011b) Biological versus physical mixing effects on benthic food web dynamics. PLoS ONE 6(3):e18078

Camargo MG (2006) SysGran: um sistema de código aberto para análises granulométricas do sedimento. Rev bras geocienc 36(2):371–378

Carver RE (1971) Procedures in sedimentary petrology. Wiley, New York

Clarke KR, Gorley RN (2006) Primer v6: user manual/tutorial. PRIMER-E, Plymouth

Fegley SR (1987) Experimental variation of near-bottom current speeds and its effects on depth distribution of sand living meiofauna. Mar Biol 95:183–191

Franco MA, Soetaert K, Costa MJ, Vincx M, Vanaverbeke J (2008) Uptake of phytodetritus by meiobenthos using ^{13}C labelled diatoms and *Phaeocystis* in two contrasting sediments from North Sea. J Exp Mar Biol Ecol 362:1–8

Gallucci F, Netto SA (2004) Effects of the passage of cold fronts over a coastal site: an ecosystem approach. Mar Ecol Prog Ser 281:79–92

Gallucci F, Steyaert M, Moens T (2005) Can field distributions of marine nematodes predacious be explained by sediment constraints on their foraging success? Mar Ecol Prog Ser 304:167–178

Gingold R, Ibarra-Obando SE, Rocha-Olivares A (2011) Spatial aggregation patterns of free-living marine nematodes in contrasting sandy beach micro-habitats. J Mar Biol Assoc UK 91:615–622

Gray J, Lissmann HW (1964) The locomotion of nematodes. J Exp Biol 41:135–154

Lana PC (2003) As marismas da baía de Paranaguá: características gerais, modos de apropriação e implicações para a legislação ambiental. Desenvolvimento e Meio Ambiente 8:11–23

Lana PC, Marone E, Lopes RM, Machado EC (2001) The Subtropical Estuarine Complex of Paranaguá Bay, Brazil. Coast Marine Ecosyst Latino Am 131:145

Lorenzen CJ (1967) Determination of chlorophyll and phaeopigments: spectrometric equations. Limnol Oceanogr 12:343–346

Maria TF, Vanaverbeke J, Esteves AM, De Troch M, Vanreusel A (2012) The importance of biological interactions for the vertical distribution of nematodes in a temperate ultra-dissipative sandy beach. Estuar Coast Shelf Sci 97:114–126

Mitbavkar S, Anil AC (2004) Vertical migratory rhythms of benthic diatoms in a tropical intertidal sand flat: influence of irradiance and tides. Mar Biol 145:9–20

Moens T, Verbeeck L, de Maeyerl A, Swings J, Vincx M (1999) Selective attraction of marine bacterivorous nematodes to their bacterial food. Mar Ecol Prog Ser 176:165–178

Moens T, Bouillon S, Gallucci F (2005) Dual stable isotope abundances unravel trophic position of estuarine nematodes. J Mar Biol Assoc UK 85:1401–1407

Noernberg MA, Lautert LFC, Araújo AD, Marone E, Angelotti R, Netto Jr JPB, Krug LA (2006) remote sensing and GIS integration for modelling the paranaguá estuarine complex—Brazil. J Coast Res SI 39. In: Proceedings of the 8th international coastal symposium, pp 1627–1631

Ólafsson E (1992) Small-scale spatial distribution of marine meiobenthos: the effects of decaying macrofauna. Oecologia 92:37–42

Ólafsson E, Ullberg J, Arroyo NL (2005) The clam *Macoma balthica* prevents in situ growth of microalgal mats: implications for meiofaunal assemblages. Mar Ecol Prog Ser 298:179–188

Palmer MA, Molloy RM (1986) Water flow and the vertical distribution of meiofauna: a flume experiment. Estuaries 9(3):225–228

Pinckney J, Sandulli R (1990) Spatial autocorrelation analysis of meiofaunal and microalgal populations on a intertidal sandflat: scale linkage between consumers and resources. Estuar Coast Shelf Sci 30:341–353

Pinto TK, Austen MC, Bemvenuti CE (2006) Effects of macroinfauna sediment disturbance on nematode vertical distribution. J Mar Biol Assoc UK 86:227–233

Platt HM, Warwick RM (1983) Free-living marine nematodes. Part I: British enoplids. Synopses of the British fauna (new series) 28

Platt HM, Warwick RM (1988) Free-living marine nematodes. Part II: British chromadorids. Synopses of the British fauna (new series) 38

Saburova MA, Polikarpov IG (2003) Diatom activity within soft sediments: behavioural and physiological processes. Mar Ecol Prog Ser 251:115–126

Santos GAP, Derycke S, Fonsêca-Genevois VG, Coelho LCBB, Correia MTS, Moens T (2008) Differential effects of food availability on population growth and fitness of three species of estuarine, bacterial-feeding nematodes. J Exp Mar Biol Ecol 355:27–40

Schratzberger M, Warr K, Rogers SI (2007) Functional diversity of nematode communities in the southwestern North Sea. Mar Environ Res 63:368–389

Soetaert K, Muthumbi A, Heip C (2002) Size and shape of ocean margin nematodes: morphological diversity and depth-related patterns. Mar Ecol Prog Ser 242:179–193

Somerfield PJ, Warwick RM (1996) Meiofauna in marine pollution monitoring programmes: a laboratory manual. MAFF Directorate of Fisheries Research Technical Series

Somerfield PJ, Dashfield SL, Warwick RM (2007) Three-dimensional spatial structure: nematodes in a sandy tidal flat. Mar Ecol Prog Ser 336:177–186

Steyaert M, Herman PMJ, Moens T, Widdows J, Vincx M (2001) Tidal migration of nematodes on an estuarine tidal flat (the Molenplaat, Schelde Estuary, SW Netherlands). Mar Ecol Prog Ser 224:209–304

Steyaert M, Vanaverbeke J, Vanreusel A, Barranguet C, Lucas C, Vincx M (2003) The importance of fine-scale, vertical profiles in characterising nematode community structure. Estuar Coast Shelf Sci 58:353–366

Steyaert M, Moodley L, Vanaverbeke J, Vandewiele S, Vincx M (2005) Laboratory experiments on the infaunal activity of intertidal nematodes. Hydrobiologia 540:217–223

Strickland JHD, Parsons TR (1972) A practical handbook of seawater analysis, 2nd edn. Fisheries Research Board of Canada, Ottawa

Ter Braak CJF, Smilauer P (1998) CANOCO release 4 reference manual and user's guide to Canoco for windows—software for canonical community ordination. Microcomputer Power, Ithaca 352

Thistle D, Sherman KM (1985) The nematode fauna of a deep-sea site exposed to strong near-bottom currents. Deep-Sea Res 32:1077–1088

Thistle D, Lambshead PJD, Sherman KM (1995) Nematode tail-shape groups respond to environmental differences in the deep sea. Vie et Milieu 45:107–115

Thomas MC, Lana PC (2011) A new look about nematodes dispersal. Zoologia, no prelo

Vanaverbeke J, Soetaert K, Vincx M (2004) Changes in morphometric characteristics of nematode communities during a spring phytoplankton bloom deposition. Mar Ecol Prog Ser 273:139–146

Wallace HR (1968) The dynamics of nematode movement. Annu Rev Phytopathol 6:91–114

Warwick RM, Platt HM, Somerfield PJ (1998) Free-living marine nematodes. Part III: monhysterids. Synopses of the British fauna (new series) 53

Wieser W (1953) Die Beziehung zwischen Mundhöhlengestalt, Ernährungs weise und Vorkommen bei freilebenden marinen Nematoden. Arkiv för Zoologi 4:439–484